Supplemental Information

1. Supplemental Figures (S1-S6)
2. Supplemental Tables (S1-S8)
3. Extended Materials and Methods
4. Supplemental References

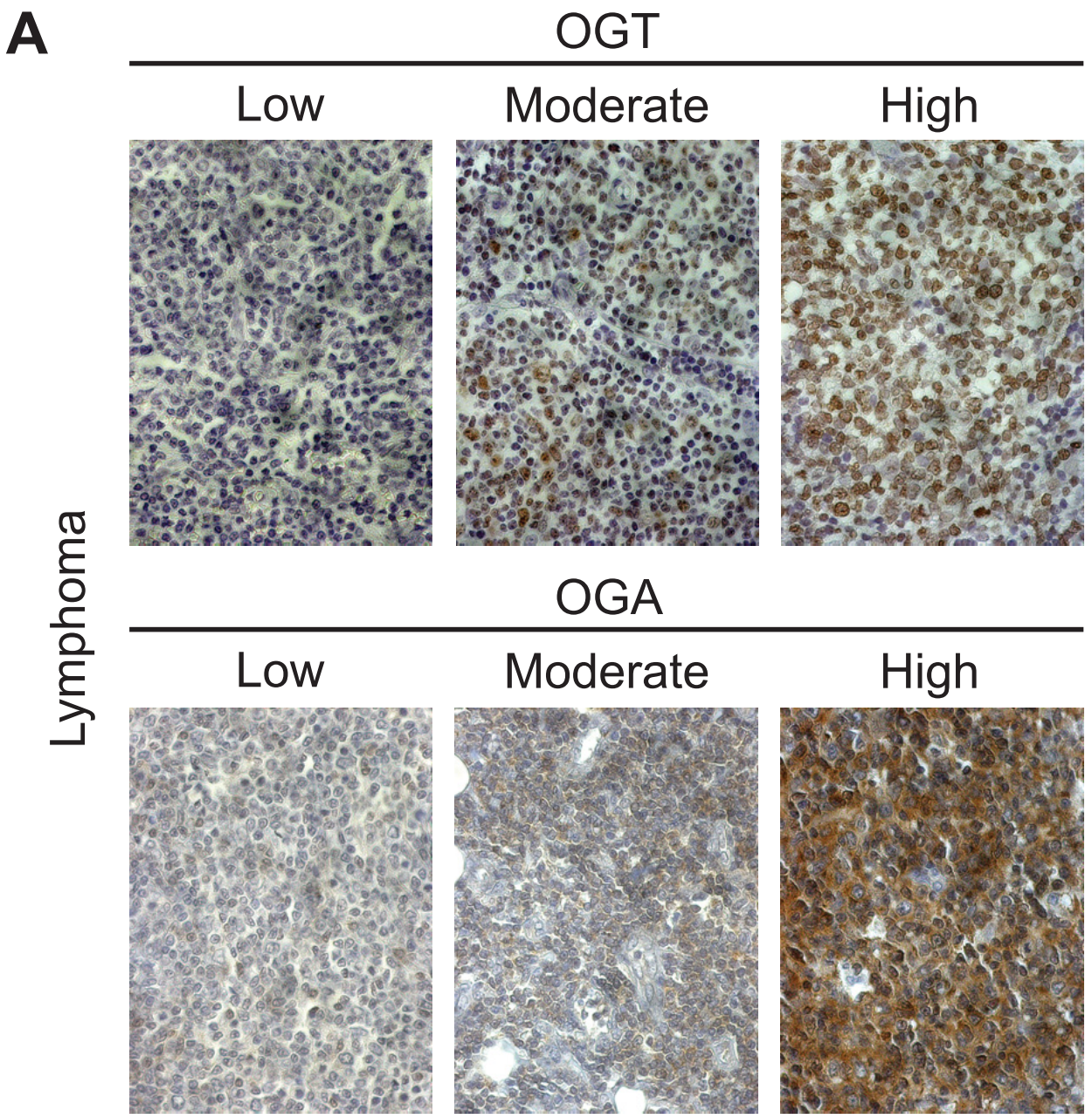
A
OGT
Low
Moderate
High
Lymphoma
OGA
Low
Moderate
High

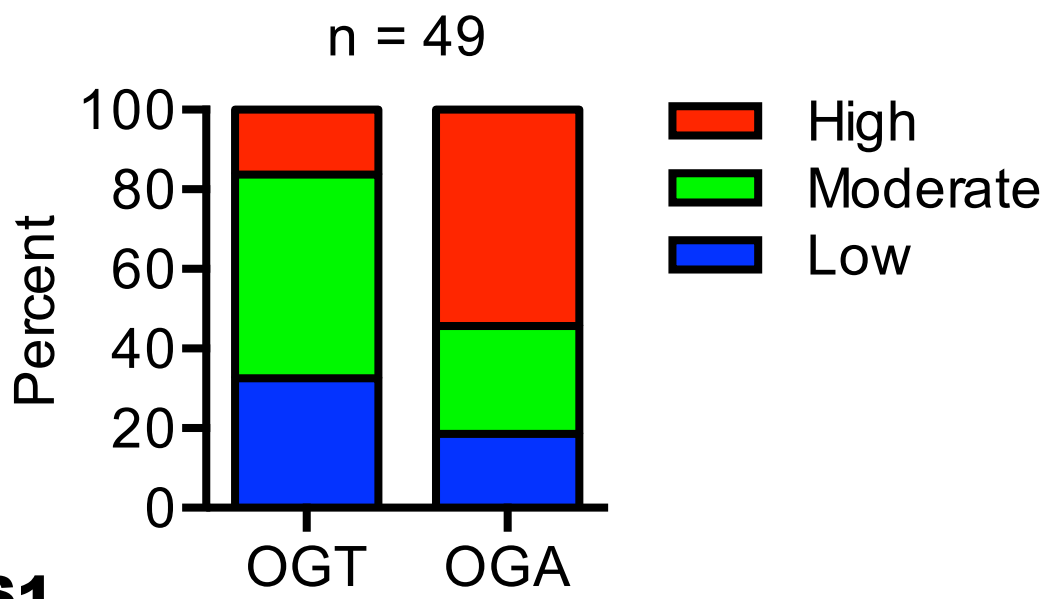
B
n = 49
100
80
60
40
20
0
Percent
OGT
OGA
High
Moderate
Low

Fig. S1

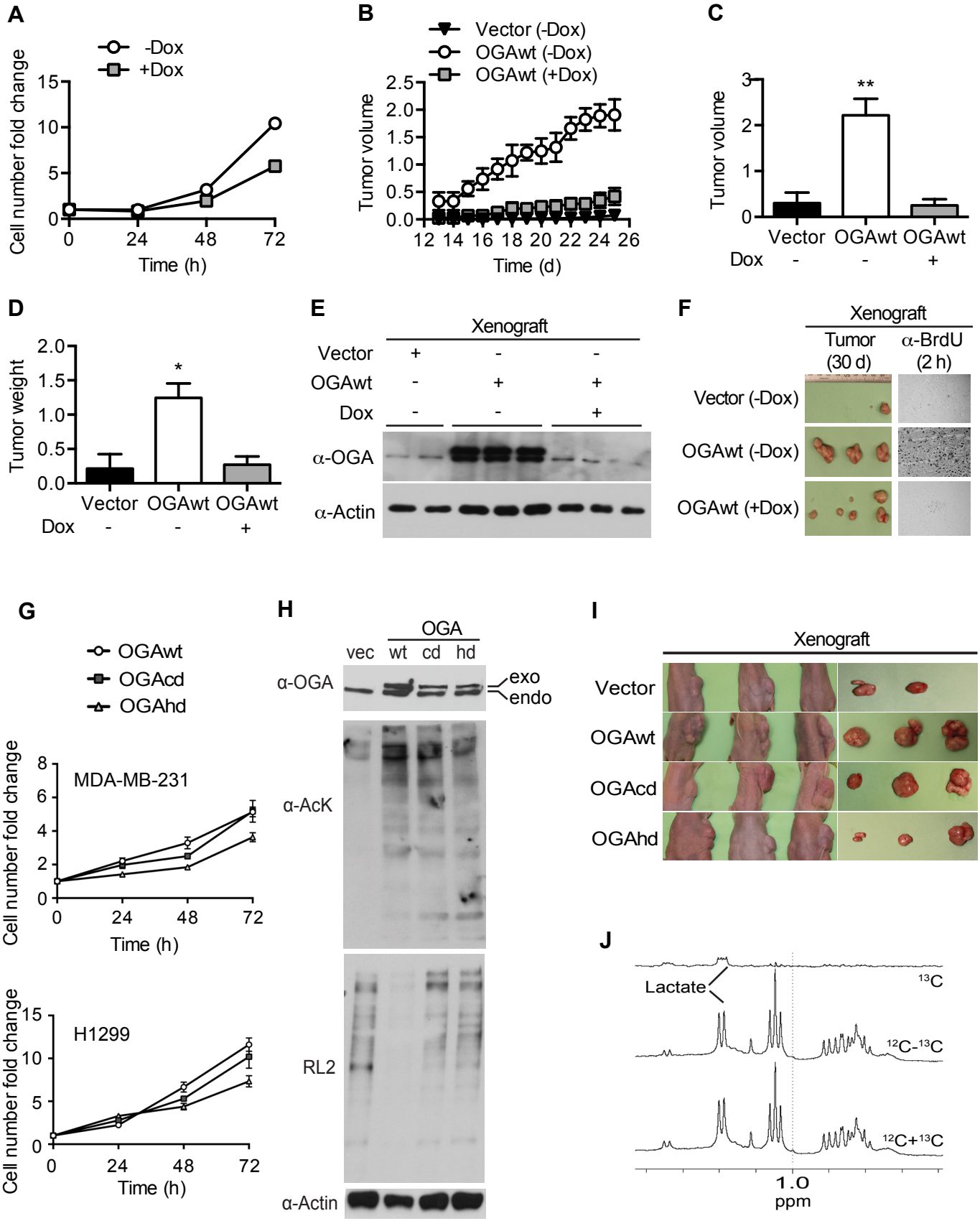
A
-Dox
+Dox
Cell number fold change
Time (h)
B
Vector (-Dox)
OGAwt (-Dox)
OGAwt (+Dox)
Tumor volume
Time (d)
C
Tumor volume
Vector
OGAwt
OGAwt
Dox
D
Tumor weight
Vector
OGAwt
OGAwt
Dox
E
Xenograft
Vector
OGAwt
Dox
α-OGA
α-Actin
F
Xenograft
Tumor (30 d)
α-BrdU (2 h)
Vector (-Dox)
OGAwt (-Dox)
OGAwt (+Dox)
G
OGAwt
OGAcd
OGAhd
MDA-MB-231
Cell number fold change
Time (h)
H1299
H
OGA
vec
wt
cd
hd
α-OGA
exo
endo
α-AcK
RL2
α-Actin
I
Xenograft
Vector
OGAwt
OGAcd
OGAhd
J
Lactate
13C
12C-13C
12C+13C
1.0
ppm

Fig. S2

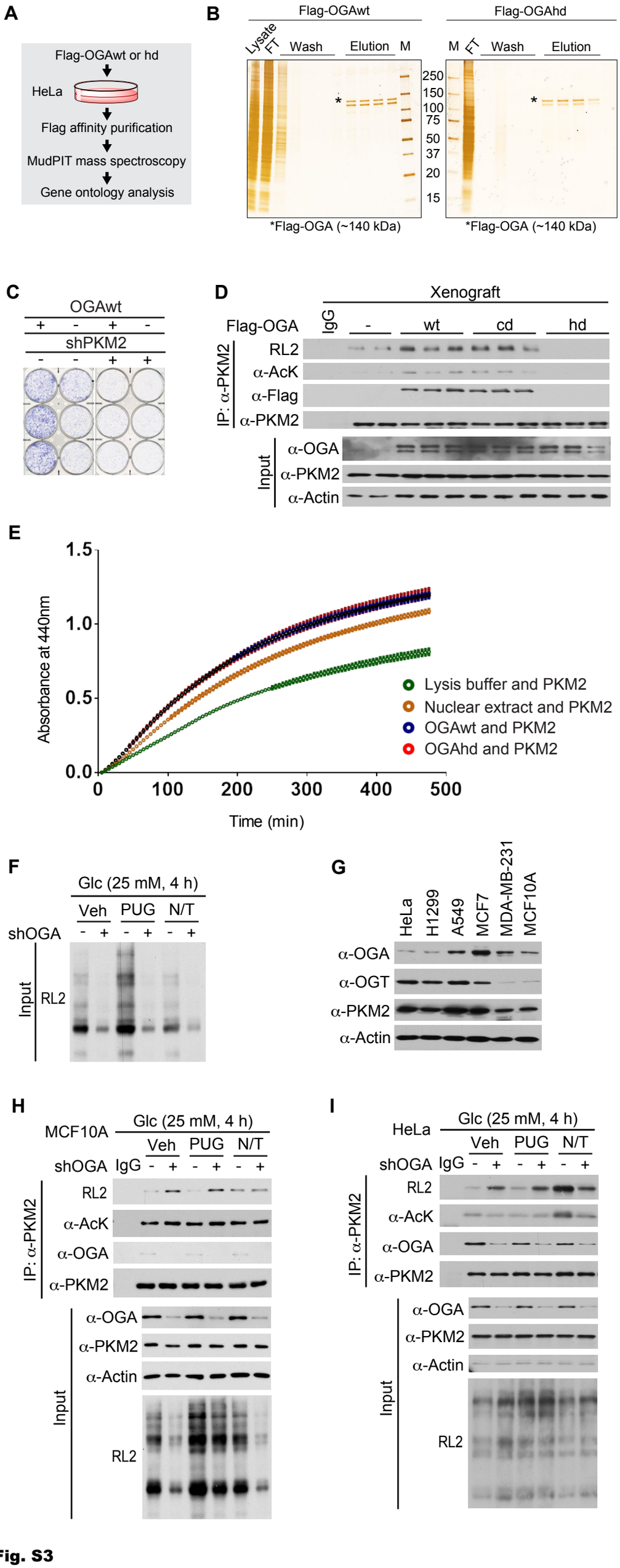
A
Flag-OGAwt or hd
HeLa
Flag affinity purification
MudPIT mass spectroscopy
Gene ontology analysis
B
Flag-OGAwt
Flag-OGAhd
Lysate
FT
Wash
Elution
M
250
150
100
75
50
37
20
15
*Flag-OGA (~140 kDa)
C
OGAwt
shPKM2
D
Xenograft
Flag-OGA
IgG
wt
cd
hd
IP: α-PKM2
RL2
α-AcK
α-Flag
α-PKM2
Input
α-OGA
α-Actin
E
Absorbance at 440nm
Time (min)
Lysis buffer and PKM2
Nuclear extract and PKM2
OGAwt and PKM2
OGAhd and PKM2
F
Glc (25 mM, 4 h)
Veh
PUG
N/T
shOGA
G
HeLa
H1299
A549
MCF7
MDA-MB-231
MCF10A
α-OGA
α-OGT
α-PKM2
α-Actin
H
MCF10A
I
HeLa

Fig. S3

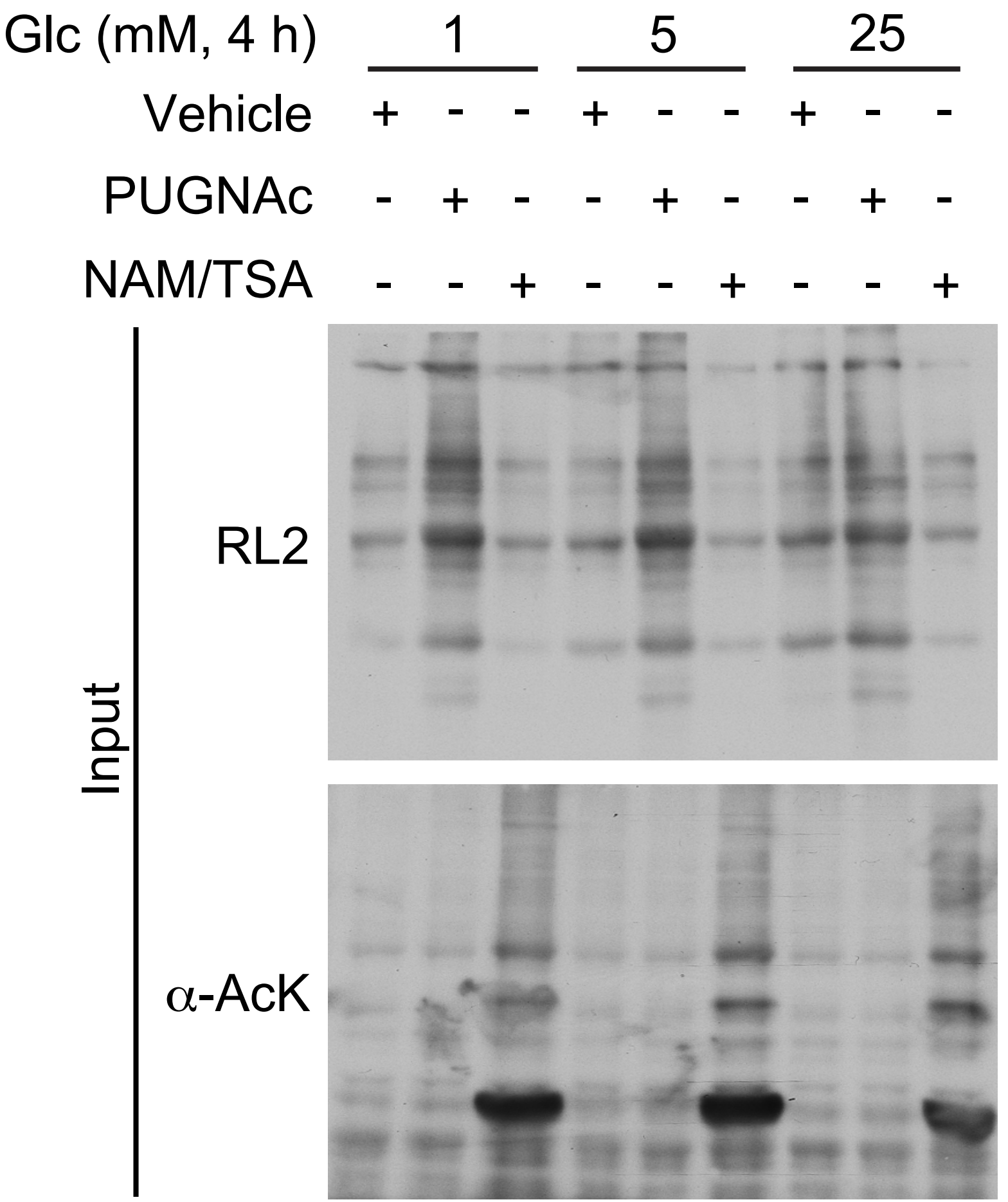

Fig. S4

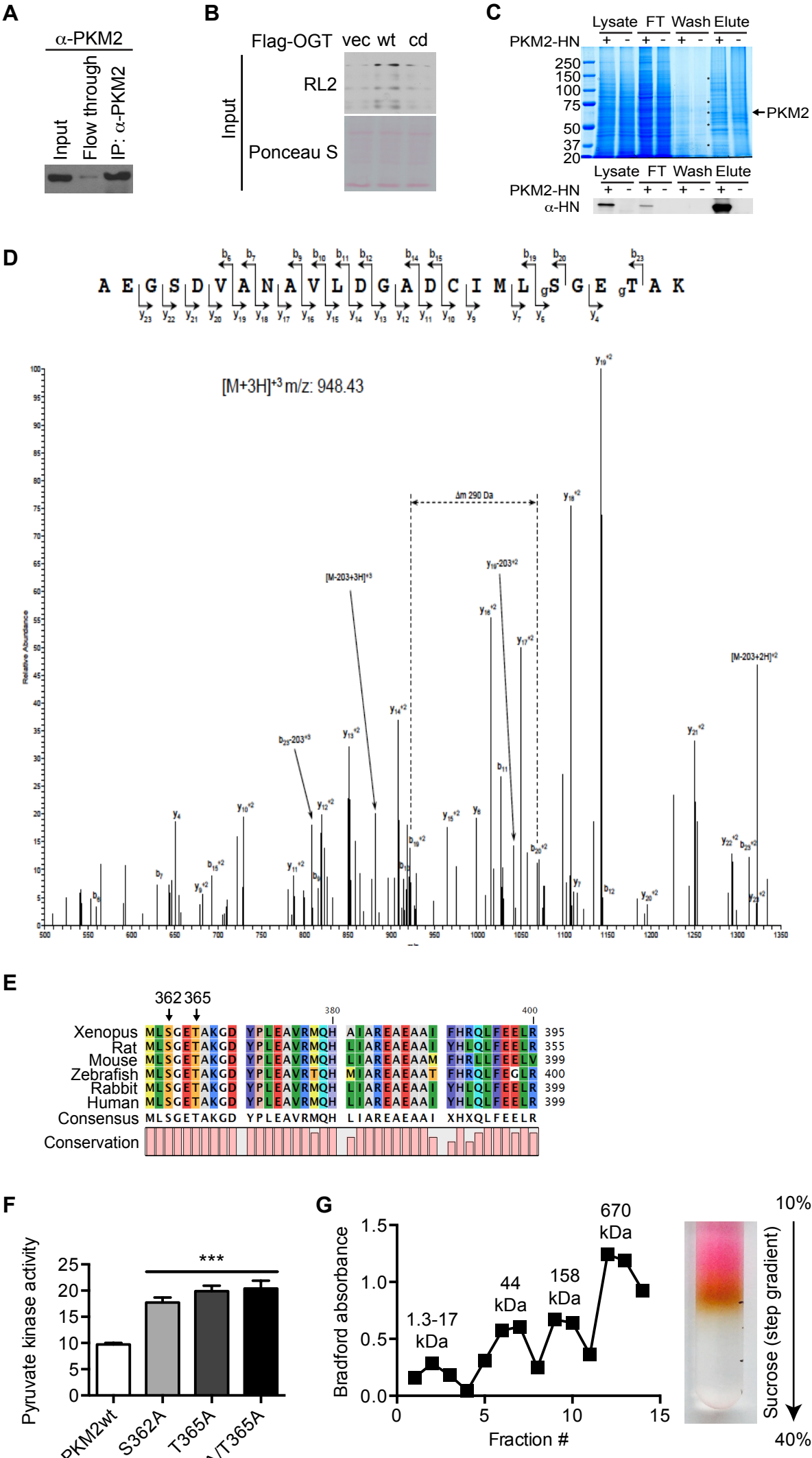
A
α-PKM2
Input
Flow through
IP: α-PKM2
B
Flag-OGT vec wt cd
Input
RL2
Ponceau S
C
Lysate FT Wash Elute
PKM2-HN
250
150
100
75
50
37
20
PKM2
α-HN
D
A E G S D V A N A V L D G A D C I M L gS G E gT A K
[M+3H]+3 m/z: 948.43
Δm 290 Da
Relative Abundance
E
362 365
Xenopus MLSGETAKGD YPLEAVRMQH AIAREAEAAI FHRQLFEELR 395
Rat MLSGETAKGD YPLEAVRMQH LIAREAEAAI YHLQLFEELR 355
Mouse MLSGETAKGD YPLEAVRMQH LIAREAEAAM FHRLLFEELV 399
Zebrafish MLSGETAKGD YPLEAVRTQH MIAREAEAAT FHRQLFEGLR 400
Rabbit MLSGETAKGD YPLEAVRMQH LIAREAEAAI YHLQLFEELR 399
Human MLSGETAKGD YPLEAVRMQH LIAREAEAAI YHLQLFEELR 399
Consensus MLSGETAKGD YPLEAVRMQH LIAREAEAAI XHXQLFEELR
Conservation
F
Pyruvate kinase activity
***
PKM2wt
S362A
T365A
S362A/T365A
G
Bradford absorbance
1.3-17 kDa
44 kDa
158 kDa
670 kDa
Fraction #
10%
Sucrose (step gradient)
40%

Fig. S5

A

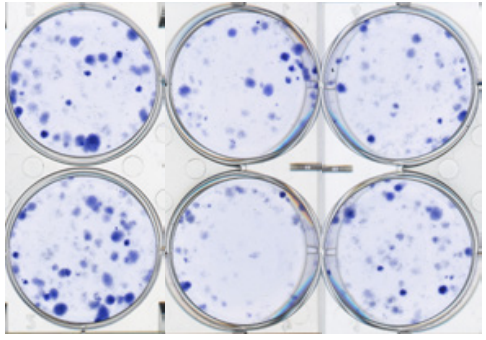

PKM2wt S362A T365A

B

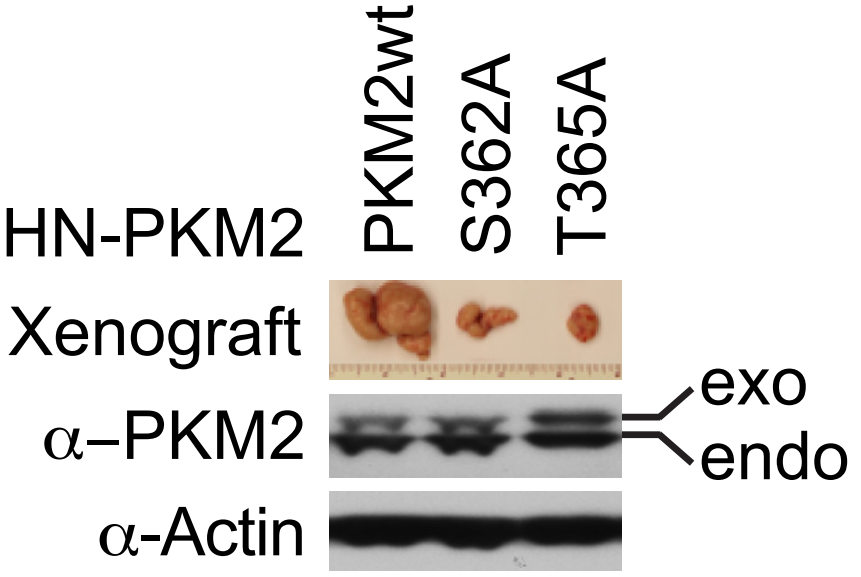

Fig. S6

Figure S1 (related to Figure 1). (A) Representative images of immunohistochemical analysis of OGT and OGA expression levels in lymphomas (magnification: 40X). **(B)** Stratification of lymphomas into low, moderate, and high expression of OGT or OGA.

Figure S2 (related to Figure 2). (A) Cell number fold change of Tet-Off HeLa cells overexpressing OGA without and with doxycycline over 72 hours (n = 6). **(B)** HeLa cells expressing vector were injected subcutaneously into the flanks of nude mice without doxycycline feeding. HeLa cells overexpressing OGA were injected subcutaneously into the flanks of nude mice without and with doxycycline feeding. Daily progression of the xenograft tumors is shown (n = 3). **(C)** Volume and **(D)** weight of the xenograft tumors at the end of the 25-day period (n = 3). **(E)** Western blot analysis of xenograft tumor homogenate confirming overexpression of OGA and silencing of OGA overexpression with doxycycline. **(F)** Images of the isolated xenograft tumors and representative images of BrdU incorporation. **(G)** Cell number fold change of MDA-MB-231 and H1299 stable cell lines expressing OGAwt, OGAcd, or OGAhd over 72 hours (n = 6). **(H)** Western blot analysis of Tet-Off HeLa cells expressing vector, OGAwt, OGAcd, or OGAhd. Endogenous and exogenous OGA are labeled. **(I)** Images of vector, OGAwt, OGAcd, and OGAhd xenograft tumors before and after surgical removal. **(J)** Representative ^{1}H-[^{13}C] NMR (POCE) spectra of HeLa cell metabolite extracts. (Top trace) ^{13}C difference spectrum obtained by subtracting the (middle trace) ^{13}C-inverted (^{12}C - ^{13}C) spectrum from the (bottom trace) non-inverted (^{12}C + ^{13}C) total spectrum. All values represent mean ± SEM. For C-D, ordinary one-way ANOVA plus Tukey's multiple comparisons test was used to compare each column with every other column (*$p < 0.05$, **$p < 0.01$ as compared to vector/-Dox and OGAwt/+Dox).

Figure S3 (related to Figure 3). (A) Schematic representation of the experimental procedure used for differential proteomic analysis of OGA-binding proteins. **(B)** Silver stains confirming

purification of Flag-OGA. **(C)** Images of crystal violet staining for clonogenic assay of HeLa cells expressing OGAwt and infected with lentivirus encoding shPKM2. **(D)** Western blot analysis of immunoprecipitated PKM2 in vector, OGAwt, OGAcd, and OGAhd xenograft tumor homogenate. **(E)** *In vitro* acetyltransferase activity assay using 2 μg OGAwt or OGAhd expressed in and purified from HEK293T cells and 2 μmol recombinant PKM2 (n = 3). HeLa cell nuclear extract was used as a positive control for acetyltransferase activity. All values represent mean ± SD. **(F)** MCF7 cells were infected with adenovirus encoding shOGA and treated with 25 mM glucose plus the indicated inhibitors for 4 hours. Whole cell lysates were analyzed by Western blotting with the RL2 antibody. **(G)** Comparison of basal OGA, OGT, and PKM2 expression levels among six cell lines by Western blotting with the indicated antibodies. **(H)** MCF10A and **(I)** HeLa cells were infected with adenovirus encoding shOGA and treated with 25 mM glucose plus the indicated inhibitors for 4 hours. PKM2 was immunoprecipitated and analyzed by Western blotting with the indicated antibodies.

Figure S4 (related to Figure 4). HeLa cells were treated with the indicated glucose concentrations plus the indicated inhibitors for 4 hours. Whole cell lysates were analyzed by Western blotting with the indicated antibodies.

Figure S5 (related to Figure 5). (A) Western blot analysis of PKM2 immunoprecipitation efficiency. **(B)** HeLa cells were transiently transfected with the indicated plasmids. Whole cell lysates were analyzed by Western blotting with the RL2 antibody. **(C)** Coomassie blue stain and Western blot confirming purification of HN-PKM2. **(D)** Representative CID-MS spectrum of purified HN-PKM2. **(E)** PKM2 amino acid sequence alignment. PKM2 O-GlcNAcylation sites identified by CID-MS are labeled. **(F)** Pyruvate kinase activity in HeLa cells transiently transfected with the indicated plasmids (n = 4). All values represent mean ± SEM. Ordinary one-way ANOVA plus Tukey's multiple comparisons test was used to compare each column with

every other column (***p < 0.001 as compared to PKM2wt). **(G)** (Left) Separation of native protein molecular weight markers by sucrose density gradient ultracentrifugation. Individual peaks and their respective molecular weight markers are labeled. (Right) Image of sucrose density gradient after ultracentrifugation. 1.3 and 17 kDa markers are colored.

Figure S6 (related to Figure 6). (A) Image of crystal violet staining for clonogenic assay of HeLa cells expressing PKM2wt, S362A, or T365A. **(B)** (Top) Representative image of isolated PKM2wt, S362A, and T365A xenograft tumors. (Bottom) Western blot analysis of endogenous and exogenous PKM2 using the indicated antibodies.

Table S1: Cancer vs. Normal Comparison of OGT mRNA expression

Comparison	Fold change	p
Chronic Lymphocytic Leukemia vs. Normal (Haferlach Leukemia)	2.039	1.48E-48
Myxoid/Round Cell Liposarcoma vs. Normal (Barretina Sarcoma)	4.056	2.05E-13
Prostate Carcinoma vs. Normal (Grasso Prostate)	2.091	1.53E-12
Mixed Germ Cell Tumor, NOS vs. Normal (Korkola Seminoma)	2.574	5.08E-11
Colorectal Carcinoma vs. Normal (Hong Colorectal)	1.749	1.43E-10
Prostate Carcinoma vs. Normal (Yu Prostate)	1.589	2.99E-10
Cirrhosis vs. Normal (Mas Liver)	1.755	5.92E-10
Pleomorphic Liposarcoma vs. Normal (Barretina Sarcoma)	2.278	9.32E-10
Colon Carcinoma vs. Normal (Skrzypczak Colorectal 2)	2.311	1.78E-09
Embryonal Carcinoma, NOS vs. Normal (Korkola Seminoma)	2.926	2.63E-09
Seminoma, NOS vs. Normal (Korkola Seminoma)	2.483	1.03E-08
Chronic Lymphocytic Leukemia vs. Normal (Basso Lymphoma)	1.762	2.48E-08
Multiple Myeloma vs. Normal (Zhan Myeloma)	1.672	2.67E-08
Teratoma, NOS vs. Normal (Korkola Seminoma)	3.208	4.83E-08
B-Cell Acute Lymphoblastic Leukemia vs. Normal (Andersson Leukemia)	1.766	6.44E-08
Angioimmunoblastic T-Cell Lymphoma vs. Normal (Piccaluga Lymphoma)	1.821	4.42E-07
Glioblastoma vs. Normal (Murat Brain)	1.349	4.59E-07
Glioblastoma vs. Normal (Shai Brain)	1.334	4.65E-07
Prostate Adenocarcinoma vs. Normal (Wallace Prostate)	2.811	7.95E-07
Infiltrating Bladder Urothelial Carcinoma vs. Normal (Sanchez-Carbayo Bladder 2)	1.451	1.01E-06
Head and Neck Squamous Cell Carcinoma vs. Normal (Ginos Head-Neck)	1.481	1.83E-06
Chronic Lymphocytic Leukemia vs. Normal (Haslinger Leukemia)	2.9	3.22E-06
Superficial Bladder Cancer vs. Normal (Dyrskjot Bladder 3)	1.8	5.20E-06
Colorectal Carcinoma vs. Normal (Skrzypczak Colorectal)	1.402	7.48E-06
Pleural Malignant Mesothelioma vs. Normal (Gordon Mesothelioma)	1.829	1.01E-05
Prostate Carcinoma vs. Normal (Arredouani Prostate)	2.267	2.05E-05
Monoclonal Gammopathy of Undetermined Significance vs. Normal (Zhan Myeloma 3)	1.559	3.31E-05
Salivary Gland Adenoid Cystic Carcinoma vs. Normal (FriersonHF Salivary-gland)	2.55	5.72E-05
Prostate Carcinoma vs. Normal (Varambally Prostate)	1.771	6.66E-05
Benign Melanocytic Skin Nevus vs. Normal (Talantov Melanoma)	1.749	8.13E-05
Hepatocellular Carcinoma vs. Normal (Wurmbach Liver)	1.905	9.27E-05
Tall Cell Variant Thyroid Gland Papillary Carcinoma vs. Normal (Giordano Thyroid)	1.245	9.47E-05
Invasive Breast Carcinoma vs. Normal (Gluck Breast)	1.656	1.37E-04
Lung Adenocarcinoma vs. Normal (Hou Lung)	1.365	1.37E-04
Round Cell Liposarcoma vs. Normal (Detwiller Sarcoma)	2.752	1.46E-04
Lung Adenocarcinoma vs. Normal (Su Lung)	1.525	1.86E-04
Gastric Mixed Adenocarcinoma vs. Normal (DErrico Gastric)	2.09	2.61E-04
Renal Pelvis Urothelial Carcinoma vs. Normal (Jones Renal)	1.983	3.03E-04
Prostate Carcinoma Epithelia vs. Normal (Tomlins Prostate)	1.643	6.11E-04
Prostate Carcinoma vs. Normal (Taylor Prostate 3)	1.23	6.95E-04
Adrenal Cortex Adenoma vs. Normal (Giordano Adrenal 2)	1.107	0.001

Lung Adenocarcinoma vs. Normal (Landi Lung)	1.242	0.001
Hepatocellular Adenoma vs. Normal (Chen Liver)	1.336	0.002
Lung Adenocarcinoma vs. Normal (Beer Lung)	1.636	0.002
Lung Adenocarcinoma vs. Normal (Stearman Lung)	1.389	0.002
Cirrhosis vs. Normal (Wurmbach Liver)	1.588	0.002
Ovarian Serous Adenocarcinoma vs. Normal (Yoshihara Ovarian)	1.586	0.002
Anaplastic Astrocytoma vs. Normal (Beroukhim Brain)	1.325	0.003
Gastric Cancer vs. Normal (Wang Gastric)	1.49	0.003
Prostate Carcinoma vs. Normal (Welsh Prostate)	1.239	0.005
Prostate Carcinoma vs. Normal (Lapointe Prostate)	1.168	0.005
Acute Myeloid Leukemia vs. Normal (Stegmaier Leukemia)	1.496	0.006
Invasive Ductal Breast Carcinoma Stroma vs. Normal (Karnoub Breast)	1.511	0.009
Prostate Carcinoma vs. Normal (Luo Prostate 2)	6.554	0.01
Prostate Carcinoma vs. Normal (Liu Prostate)	1.362	0.015
B-Cell Childhood Acute Lymphoblastic Leukemia vs. Normal (Coustan-Smith Leukemia)	1.635	0.028
Esophageal Adenocarcinoma vs. Normal (Kimchi Esophagus)	1.47	0.046
Squamous Cell Lung Carcinoma vs. Normal (Bhattacharjee Lung)	1.503	0.076
Barrett's Esophagus vs. Normal (Hao Esophagus)	1.244	0.104
Tongue Squamous Cell Carcinoma vs. Normal (Ye Head-Neck)	1.039	0.127
Myelodysplastic Syndrome vs. Normal (Haferlach Leukemia)	2.039	0.155
Prostate Carcinoma vs. Normal (Holzbeierlein Prostate)	1.142	0.222
Barrett's Esophagus vs. Normal (Kim Esophagus)	1.078	0.229

Table S2: Cancer vs. Normal Comparison of OGA mRNA expression

Comparison	Fold change	p
Chronic Lymphocytic Leukemia vs. Normal (Haferlach Leukemia)	1.559	9.50E-25
Cirrhosis vs. Normal (Mas Liver)	1.682	1.27E-10
Monoclonal Gammopathy of Undetermined Significance vs. Normal (Zhan Myeloma 3)	1.788	8.66E-08
Superficial Bladder Cancer vs. Normal (Dyrskjot Bladder 3)	1.823	1.35E-07
Pancreatic Ductal Adenocarcinoma vs. Normal (Badea Pancreas)	1.51	2.99E-06
Colon Carcinoma Epithelia vs. Normal (Skrzypczak Colorectal 2)	1.41	1.44E-05
Angioimmunoblastic T-Cell Lymphoma vs. Normal (Piccaluga Lymphoma)	1.69	1.87E-05
Colon Carcinoma vs. Normal (Skrzypczak Colorectal 2)	1.633	2.06E-05
Clear Cell Renal Cell Carcinoma vs. Normal (Gumz Renal)	2.399	4.32E-05
Gastric Mixed Adenocarcinoma vs. Normal (DErrico Gastric)	2.975	6.17E-05
Acute Myeloid Leukemia vs. Normal (Stegmaier Leukemia)	2.462	1.25E-04
Hepatocellular Carcinoma vs. Normal (Wurmbach Liver)	1.452	2.91E-04
Adrenal Cortex Adenoma vs. Normal (Giordano Adrenal 2)	1.131	3.02E-04
Prostate Adenocarcinoma vs. Normal (Wallace Prostate)	1.503	4.64E-04
Papillary Renal Cell Carcinoma vs. Normal (Yusenko Renal)	1.529	5.27E-04
Cirrhosis vs. Normal (Wurmbach Liver)	1.996	7.68E-04
Head and Neck Squamous Cell Carcinoma vs. Normal (Ginos Head-Neck)	1.487	0.001
Invasive Ductal Breast Carcinoma Stroma vs. Normal (Karnoub Breast)	1.873	0.002
Oropharyngeal Carcinoma vs. Normal (Pyeon Multi-cancer)	2.076	0.002
Oligodendroglioma vs. Normal (Shai Brain)	2.212	0.003
Salivary Gland Adenoid Cystic Carcinoma vs. Normal (FriersonHF Salivary-gland)	1.739	0.003
Gastric Cancer vs. Normal (Wang Gastric)	1.331	0.003
Round Cell Liposarcoma vs. Normal (Detwiller Sarcoma)	2.354	0.004
Ductal Breast Carcinoma in Situ Epithelia vs. Normal (Ma Breast 4)	1.732	0.004
Prostate Carcinoma vs. Normal (Arredouani Prostate)	1.333	0.006
Pleomorphic Liposarcoma vs. Normal (Detwiller Sarcoma)	2.316	0.007
Pleural Malignant Mesothelioma vs. Normal (Gordon Mesothelioma)	2.912	0.007
Cervical Squamous Cell Carcinoma Epithelia vs. Normal (Zhai Cervix)	1.327	0.01
Ovarian Clear Cell Adenocarcinoma vs. Normal (Hendrix Ovarian)	1.121	0.01
Dedifferentiated Liposarcoma vs. Normal (Detwiller Sarcoma)	1.67	0.011
Skin Squamous Cell Carcinoma vs. Normal (Nindl Skin)	1.364	0.016
Tall Cell Variant Thyroid Gland Papillary Carcinoma vs. Normal (Giordano Thyroid)	1.079	0.02
Benign Melanocytic Skin Nevus vs. Normal (Talantov Melanoma)	2.286	0.029
Invasive Mixed Breast Carcinoma vs. Normal (Radvanyi Breast)	2.507	0.032
Chronic Lymphocytic Leukemia vs. Normal (Haslinger Leukemia)	1.36	0.039
Benign Prostatic Hyperplasia Stroma vs. Normal (Tomlins Prostate)	1.547	0.053
Prostate Carcinoma vs. Normal (Liu Prostate)	1.081	0.059
Ovarian Mucinous Adenocarcinoma vs. Normal (Lu Ovarian)	1.139	0.09
Hepatocellular Adenoma vs. Normal (Chen Liver)	1.18	0.095
Prostate Carcinoma vs. Normal (Luo Prostate 2)	1.177	0.102

Table S3: Cancer vs. Normal Comparison of GFPT1 mRNA expression

Comparison	Fold change	p
Lung Adenocarcinoma vs. Normal (Beer Lung)	2.213	8.34E-10
Lung Adenocarcinoma vs. Normal (Bhattacharjee Lung)	1.441	0.05
Pancreatic Intraepithelial Neoplasia vs. Normal (Buchholz Pancreas)	1.181	0.025
Hepatocellular Adenoma vs. Normal (Chen Liver)	1.12	0.008
Invasive Breast Carcinoma vs. Normal (Curtis Breast)	1.64	8.10E-05
Medullary Breast Carcinoma vs. Normal (Curtis Breast)	1.514	5.20E-10
Mucinous Breast Carcinoma vs. Normal (Curtis Breast)	1.829	3.36E-13
Tubular Breast Carcinoma vs. Normal (Curtis Breast)	1.479	7.55E-16
Invasive Breast Carcinoma vs. Normal (Gluck Breast)	1.526	1.12E-04
Pancreatic Ductal Adenocarcinoma Epithelia vs. Normal (Grutzmann Pancreas)	1.829	0.014
Clear Cell Renal Cell Carcinoma vs. Normal (Gumz Renal)	1.973	1.46E-04
Myelodysplastic Syndrome vs. Normal (Haferlach Leukemia)	1.128	2.79E-08
Barrett's Esophagus vs. Normal (Hao Esophagus)	3.345	4.79E-07
Ovarian Clear Cell Adenocarcinoma vs. Normal (Hendrix Ovarian)	1.482	1.04E-06
Chromophobe Renal Cell Carcinoma vs. Normal (Higgins Renal)	1.474	0.016
Prostate Carcinoma vs. Normal (Holzbeierlein Prostate)	1.203	0.202
Lung Adenocarcinoma vs. Normal (Hou Lung)	2.13	4.51E-14
Renal Pelvis Urothelial Carcinoma vs. Normal (Jones Renal)	2.251	1.21E-07
Rectal Mucinous Adenocarcinoma vs. Normal (Kaiser Colon)	1.564	2.64E-04
Barrett's Esophagus vs. Normal (Kim Esophagus)	2.489	3.17E-07
Barrett's Esophagus vs. Normal (Kimchi Esophagus)	2.03	0.002
Seminoma, NOS vs. Normal (Korkola Seminoma)	3.56	6.76E-08
Lung Adenocarcinoma vs. Normal (Landi Lung)	2.536	1.05E-23
Prostate Carcinoma vs. Normal (Liu Prostate)	1.253	0.001
Prostate Carcinoma vs. Normal (Luo Prostate 2)	3.536	0.021
Ductal Breast Carcinoma in Situ Epithelia vs. Normal (Ma Breast 4)	2.421	4.12E-06
Anaplastic Large Cell Lymphoma vs. Normal (Piccaluga Lymphoma)	2.208	1.46E-05
Ductal Breast Carcinoma vs. Normal (Richardson Breast 2)	2.144	5.15E-07
Prostate Carcinoma vs. Normal (Singh Prostate)	1.699	6.38E-06
Lung Adenocarcinoma vs. Normal (Stearman Lung)	1.589	1.67E-07
Prostate Carcinoma Epithelia vs. Normal (Tomlins Prostate)	2.516	2.64E-05
Acute Myeloid Leukemia vs. Normal (Valk Leukemia)	1.313	5.03E-04
Prostate Adenocarcinoma vs. Normal (Vanaja Prostate)	2.141	2.34E-04
Prostate Adenocarcinoma vs. Normal (Wallace Prostate)	1.531	0.003
Prostate Carcinoma vs. Normal (Welsh Prostate)	2.613	6.25E-05
Tongue Squamous Cell Carcinoma vs. Normal (Ye Head-Neck)	1.885	2.00E-05
Renal Oncocytoma vs. Normal (Yusenko Renal)	2.222	7.37E-04
High Grade Cervical Squamous Intraepithelial Neoplasia Epithelia vs. Normal (Zhai Cervix)	1.435	0.001
Monoclonal Gammopathy of Undetermined Significance vs. Normal (Zhan Myeloma 3)	1.609	6.33E-06

Table S4: Immunohistochemical analysis of colon adenocarcinoma (HCol-Ade180Sur-04)					
		OGA level			**p***
		Low	Moderate	High	
Total	90	8	50	32	
Gender					0.228
Male	47	4	30	13	
Female	43	4	20	19	
Pathological grade					**0.016**
I,I-II,II	54	1	32	21	
II-III,III	36	7	18	11	
Invasive depth					0.678
T1,T2	9	1	6	2	
T3,T4	81	7	44	30	
Node status					0.57
N0	65	7	36	22	
N1-N2	25	1	14	10	
Clinical stage					0.9
IA-IIA	50	5	27	18	
IIB-IV	40	3	23	14	
*Chi-square test					

Table S5: Immunohistochemical analysis of breast ductal carcinoma (HBre-Duc170Sur-01)					
		OGA level			**p***
		Low	Moderate	High	
Total	**160**	**39**	**51**	**70**	
Pathological grade					**0.008**
I,I-II	44	18	13	13	
II,II-III,III	116	21	38	57	
Invasive depth					0.571
T1	37	12	9	16	
T2	108	23	36	49	
T3	15	4	6	5	
Node status					0.956
N0	65	16	20	29	
N1,N2	94	22	31	41	
Clinical stage					0.653
I-IIB	110	28	33	49	
III	49	10	18	21	
*Chi-square test					

Table S6: Immunohistochemical analysis of lung adenocarcinoma (HLug-Ade150Sur-01)					
		OGA level			**p***
		Low	Moderate	High	
Total	75	28	31	16	
Gender					0.015
Male	39	10	16	13	
Female	36	18	15	3	
Pathological grade					0.294
I,I-II,II	53	22	22	9	
II-III,III	22	6	9	7	
Invasive depth					0.223
T1a-T2a	21	10	10	1	
T2b-T4	37	13	15	9	
Node status					0.61
N0	40	17	15	8	
N1-N2	35	11	16	8	
Clinical stage					**0.039**
IA-IB	23	12	10	1	
IIA-IV	52	16	21	15	
*Chi-square test					

Table S7: OGAwt-binding proteins

Gene description	Accession
MGEA5 Isoform 1 of Bifunctional protein NCOAT	IPI00477231.2
PRMT5 Protein arginine N-methyltransferase 5	IPI00441473.3
KRT1 Keratin, type II cytoskeletal 1	IPI00220327.3
PPM1B Isoform Beta-1 of Protein phosphatase 1B	IPI00026612.1
HSPA1B;HSPA1A heat shock 70kDa protein 1B	IPI00847536.1
RBM10 Hypothetical protein DKFZp686E2459	IPI00375731.1
ACTB Actin, cytoplasmic 2	IPI00848058.1
SCYL2 SCY1-like protein 2	IPI00396218.2
RBM10 RNA binding motif protein 10	IPI00549342.2
STK38 Serine/threonine-protein kinase 38	IPI00027251.1
KRT9 Keratin, type I cytoskeletal 9	IPI00019359.3
EIF4B eukaryotic translation initiation factor 4B	IPI00439415.6
NONO Non-POU domain-containing octamer-binding protein	IPI00304596.3
FLNA Filamin-A	IPI00333541.6
KRT10 Keratin, type I cytoskeletal 10	IPI00009865.2
TUBB Tubulin, beta polypeptide	IPI00645452.1
KRT2 Keratin, type II cytoskeletal 2 epidermal	IPI00021304.1
PFKFB3 Isoform 1 of 6-phosphofructo-2-kinase/fructose-2,6-biphosphatase 3	IPI00004511.3
EEF1A1 Elongation factor 1-alpha 1	IPI00396485.3
TUBB2C Tubulin beta-2C chain	IPI00007752.1
CLOCK Circadian locomoter output cycles protein kaput	IPI00007284.1
NCL Isoform 1 of Nucleolin	IPI00604620.3
ACTC1 Actin, alpha cardiac muscle 1	IPI00023006.1
TUBB2B Tubulin beta-2B chain	IPI00031370.3
PRPF31 Isoform 1 of U4/U6 small nuclear ribonucleoprotein Prp31	IPI00292000.6
HSPA8 Isoform 1 of Heat shock cognate 71 kDa protein	IPI00003865.1
WDR77 Methylosome protein 50	IPI00012202.1
STK38L Serine/threonine-protein kinase 38-like	IPI00237011.5
TUBB2A Tubulin beta-2A chain	IPI00013475.1
THRAP3 Thyroid hormone receptor-associated protein 3	IPI00104050.3
SFPQ Isoform Long of Splicing factor, proline- and glutamine-rich	IPI00010740.1
TUBA1B Tubulin alpha-1B chain	IPI00387144.4
BCLAF1 Isoform 1 of Bcl-2-associated transcription factor 1	IPI00006079.1
BCLAF1 Isoform 3 of Bcl-2-associated transcription factor 1	IPI00413672.1
HSPD1 60 kDa heat shock protein, mitochondrial precursor	IPI00784154.1
VIM Vimentin	IPI00418471.6
TUBA1A Tubulin alpha-1A chain	IPI00180675.4
67 kDa protein	IPI00020513.2
TUBA1C Tubulin alpha-1C chain	IPI00218343.4
SF3B2 splicing factor 3B subunit 2	IPI00221106.5
HSPA5 HSPA5 protein	IPI00003362.2
HSPA1L Heat shock 70kDa protein 1-like variant	IPI00643152.1
NT5C2 Cytosolic purine 5'-nucleotidase	IPI00029054.1

PFKFB2 Isoform 1 of 6-phosphofructo-2-kinase/fructose-2,6-biphosphatase 2	IPI00305589.3
PKM2 Isoform M2 of Pyruvate kinase isozymes M1/M2	IPI00479186.5
PKM2 58 kDa protein	IPI00784179.1
HNRPH1 HNRPH1 protein	IPI00479191.2
NPM1 Isoform 1 of Nucleophosmin	IPI00549248.4
PPIAL3;PPIA;LOC654188 Peptidyl-prolyl cis-trans isomerase A	IPI00419585.9
HSPA9 Stress-70 protein, mitochondrial precursor	IPI00007765.5
Similar to Elongation factor 1-alpha 1	IPI00180730.1

Table S8: OGAhd-binding proteins

Gene description	Accession
MGEA5 Isoform 1 of Bifunctional protein NCOAT	IPI00477231.2
MGEA5 Isoform 2 of Bifunctional protein NCOAT	IPI00181391.8
SCYL2 SCY1-like protein 2	IPI00396218.2
EIF4B eukaryotic translation initiation factor 4B	IPI00439415.6
KRT1 Keratin, type II cytoskeletal 1	IPI00220327.3
THRAP3 Thyroid hormone receptor-associated protein 3	IPI00104050.3
Eukaryotic translation elongation factor 1 alpha-like 3	IPI00472724.1
EEF1A2 Elongation factor 1-alpha 2	IPI00014424.1
Similar to Elongation factor 1-alpha 1	IPI00180730.1
HSPA1B;HSPA1A heat shock 70kDa protein 1B	IPI00847536.1
NONO Non-POU domain-containing octamer-binding protein	IPI00304596.3
KRT2 Keratin, type II cytoskeletal 2 epidermal	IPI00021304.1
KRT9 Keratin, type I cytoskeletal 9	IPI00019359.3
FLNA Filamin-A	IPI00333541.6
KRT10 Keratin, type I cytoskeletal 10	IPI00009865.2
PRPF31 Isoform 1 of U4/U6 small nuclear ribonucleoprotein Prp31	IPI00292000.6
BCLAF1 Isoform 1 of Bcl-2-associated transcription factor 1	IPI00006079.1
STK38 Serine/threonine-protein kinase 38	IPI00027251.1
TUBA1B Tubulin alpha-1B chain	IPI00387144.4
NCL Isoform 1 of Nucleolin	IPI00604620.3
31 kDa protein	IPI00479366.1
RBM10 Hypothetical protein DKFZp686E2459	IPI00375731.1
MYH9 Myosin-9	IPI00019502.3
BCLAF1 Isoform 4 of Bcl-2-associated transcription factor 1	IPI00413673.1
SFPQ Isoform Long of Splicing factor, proline- and glutamine-rich	IPI00010740.1
PPM1B Isoform Beta-1 of Protein phosphatase 1B	IPI00026612.1
DDX3X ATP-dependent RNA helicase DDX3X	IPI00215637.5
PRMT5 Protein arginine N-methyltransferase 5	IPI00441473.3
STK38L Serine/threonine-protein kinase 38-like	IPI00237011.5
HNRPK Isoform 2 of Heterogeneous nuclear ribonucleoprotein K	IPI00216746.1
SLC25A5 ADP/ATP translocase 2	IPI00007188.5
GSTO1 Glutathione transferase omega-1	IPI00019755.3
NT5C2 Cytosolic purine 5'-nucleotidase	IPI00029054.1
ASCC3L1 U5 small nuclear ribonucleoprotein 200 kDa helicase	IPI00420014.2
SLC25A6 ADP/ATP translocase 3	IPI00291467.7
IPO8 Importin-8	IPI00007401.1
LOC144097 Hypothetical protein LOC144097	IPI00106955.3
PARP1 Poly [ADP-ribose] polymerase 1	IPI00449049.5
SF3B3 Isoform 1 of Splicing factor 3B subunit 3	IPI00300371.5
SF3B4 Splicing factor 3B subunit 4	IPI00017339.1

Extended Materials and Methods

Gene expression analysis

Data for OGT, OGA, and HBP gene expression analysis were obtained from the commercially available Oncomine database (Life Technologies).

Immunohistochemistry

Tissue microarrays for colon cancer (OD-CT-DgCol03-002), breast cancer (OD-CT-RpBre03-004), lung cancer (Hlug-Ade090Lym-01), were purchased from Shanghai Outdo Biotech Company. Tissue microarray for lymphoma was obtained from the Memorial Sloan Kettering Cancer Center histology core facility. Anti-OGT (ab96718) and anti-OGA (NBP1-96679) antibodies were purchased from Abcam and Novus, respectively. Immunohistochemistry was performed as follows: after baking on a panel at 70°C, formalin-fixed paraffin-embedded tissue samples were deparaffinized with xylenes and rehydrated through gradient ethanol immersion. Endogenous peroxidase activity was quenched by incubation with 3% (v/v) hydrogen peroxide in methanol for 12 minutes, followed by three 3-minute washes with PBS. The sections were then blocked with 10% (v/v) normal goat serum in PBS for 25 minutes, followed by overnight incubation with primary antibody in a moist chamber at 4°C. Primary antibodies were diluted in PBS containing 1% (w/v) BSA and pre-immune mouse serum was substituted for primary antibody as a negative control. After three 5-minute washes with PBS, the sections were incubated with secondary antibody for 25 minutes at room temperature, followed by three additional 5-minute washes with PBS. Reaction products were visualized with diaminobenzidine (DAB, ZLI-9032, ZSGB) at room temperature. After being counterstained with Harris hematoxylin (ZLI-9039, ZSGB) for 4 minutes and rinsed with tap water, the sections were immediately dehydrated by sequential immersion in gradient ethanol and xylenes and mounted with resin and cover slips. Images were obtained using an Olympus BX51 light microscope equipped with a DP70 digital camera. For evaluation of cell staining, sections were examined by

two independent observers without prior knowledge of the clinical or clinicopathological status of the specimens. Antigen expression levels were stratified into low, moderate, or high by optical evaluation. Staining of less than 10% of the cancer cells in a core was classified as negative.

Flag-OGA affinity purification and MudPIT analysis

Flag-OGA protein complexes were purified from whole cell lysates by immunoprecipitation with anti-Flag M2 affinity gel (Sigma). Briefly, HeLa cells transiently transfected with Flag-OGA were washed twice with cold PBS, detached from culture dishes using a cell scraper, collected in 50 mL tubes, and centrifuged at 500g at 4°C to obtain cell pellets. In the cold room, cell pellets were lysed for 30 minutes in cold NETN buffer with protease and protein phosphatase inhibitors. Whole cell lysates were centrifuged at 15,000 RPM at 4°C and supernatants were collected. Flag M2 beads were activated by sequential washing with cold PBS, 100 mM glycine, and NETN buffer (three times per buffer). In the cold room, activated Flag M2 beads were incubated with whole cell lysates for 2 hours to allow the beads to capture Flag-OGA. Protein-bound beads were collected by centrifuging at 200g at 4°C and transferred to 5 mL columns for washing and elution. Flag-OGA was eluted using 100 μg/mL Flag peptide (Sigma) in washing buffer. Silver staining and Western blotting were performed to confirm the presence of Flag-OGA among the purified proteins. The purified proteins were stored at -80°C for use in acetyltransferase activity assays. For MudPIT analysis, trichloroacetic acid (TCA) precipitation and acetone washing to remove TCA were performed. MudPIT analysis was performed as described in the literature[3].

Acetyltransferase activity assay

Recombinant PKM2 was purchased from Novus. Flag-OGAwt or Flag-OGAhd was expressed in HEK293T cells and purified using a Flag affinity column. Acetyltransferase activity assay was

performed using the HAT Activity Colorimetric Assay Kit (Biovision) with OGA as the enzyme and PKM2 as the substrate.

HN-PKM2 affinity purification from mammalian cells

HEK293T cells transiently transfected with HN-PKM2 were collected using a cell scraper and lysed in a 1% Nonidet P-40, 50 mM HEPES buffer with protease, protein phosphatase, and O-GlcNAcase inhibitors. Supernatants of whole cell lysates were allowed to flow through pre-equilibrated TALON Metal Affinity Resin (Clontech). Bound protein was eluted using 200 mM imidazole and desalting columns were used for removal of imidazole and buffer exchange. Silver staining and Western blotting were performed to confirm the presence of HN-PKM2 among the purified proteins. For identification of O-GlcNAc sites by CID-MS, the purified proteins were concentrated using a 3 kDa cutoff centrifugal filter, resolved by SDS-PAGE, and stained with a Coomassie blue dye to visualize 50-75 kDa protein bands for excision.

Identification of O-GlcNAc sites by CID-MS

Protein bands were excised from Coomassie-stained gels, destained, and subjected to in-gel trypsin digestion. Briefly, digestion was performed with 12.5 ng/μL trypsin in 50 mM ammonium bicarbonate and incubated overnight at 37°C. The resulting peptides were extracted with 50% acetonitrile/5% formic acid and dried in a vacuum centrifuge. Prior to measurement, dried peptides were dissolved in 0.1% formic acid. The peptide mixtures were pressure-loaded onto a 250 micron internal diameter fused silica capillary (Polymicro Technologies) column with a Kasil frit packed with 2.5 cm of 5 micron Partisphere strong cation exchange (SCX) resin (Whatman) and 2.5 cm of 5 micron C18 resin (Phenomenex). After desalting, this bi-phasic column was connected to a 100 micron internal diameter fused silica capillary (Polymicro Technologies) analytical column with a 3 micron pulled-tip, packed with 10 cm of 3 micron C18 resin (Phenomenex). The entire three-phase column was placed inline with a 1200 quaternary HPLC

pump (Agilent) and analyzed using a modified 12-step separation as described in the literature[4]. As peptides were eluted from the microcapillary column, they were electrosprayed directly into a hybrid LTQ Orbitrap mass spectrometer (Thermo Fisher Scientific). MS instrument method consisted of an FT full-scan MS analysis (400-1600 *m/z*, 60000 resolution) followed by data-dependent MS/MS scans of the 8 most intense precursors at 35% normalized collision energy with dynamic exclusion for 60 s. Applications of mass spectrometer scan functions and HPLC solvent gradients were controlled by the Xcalibur data system (Thermo Scientific). MS/MS spectra were extracted using RawXtract (version 1.9.9)[1]. MS/MS spectra were searched using the ProLuCID algorithm against a human IPI database concatenated to a decoy database in which the sequence for each entry in the original database was reversed[2, 5]. The ProLuCID search was performed using half enzyme specificity, differential modification of serine and threonine due to O-GlcNAc (203.0794). ProLuCID search results were assembled and filtered using the DTASelect (version 2.0) algorithm. The protein identification false positive rate was kept below one percent and all peptide-spectra matches had less than 5 ppm mass error.

Supplemental References

1 McDonald WH, Tabb DL, Sadygov RG, MacCoss MJ, Venable J, Graumann J *et al*. MS1, MS2, and SQT-three unified, compact, and easily parsed file formats for the storage of shotgun proteomic spectra and identifications. Rapid communications in mass spectrometry : RCM 2004; 18: 2162-2168.

2 Peng J, Elias JE, Thoreen CC, Licklider LJ, Gygi SP. Evaluation of multidimensional chromatography coupled with tandem mass spectrometry (LC/LC-MS/MS) for large-scale protein analysis: the yeast proteome. Journal of proteome research 2003; 2: 43-50.

3 Ruan HB, Han X, Li MD, Singh JP, Qian K, Azarhoush S *et al*. O-GlcNAc transferase/host cell factor C1 complex regulates gluconeogenesis by modulating PGC-1alpha stability. Cell metabolism 2012; 16: 226-237.

4 Washburn MP, Wolters D, Yates JR, 3rd. Large-scale analysis of the yeast proteome by multidimensional protein identification technology. Nat Biotechnol 2001; 19: 242-247.

5 Xu T, Venable JD, Park SK, Cociorva D, Lu B, Liao L *et al*. ProLuCID, a fast and sensitive tandem mass spectra-based protein identification program. Molecular & Cellular Proteomics 2006; 5: S174-S174.